applied sciences

MDPI

Article

New Correlations for the Determination of Undrained Shear, Elastic Modulus, and Bulk Density Based on Dilatometer Tests (DMT) for Organic Soils in the South of Quito, Ecuador

Jorge Mayanquer [1], Mariela Anaguano-Marcillo [1], Nicolás Játiva [1] and Jorge Albuja-Sánchez [1,2,*]

[1] Faculty of Engineering, Laboratory of Materials Resistance, Soil Mechanics, Pavements and Geotechnics, Pontificia Universidad Católica del Ecuador (PUCE), Quito 170143, Ecuador; jmayanquer707@puce.edu.ec (J.M.); managuano134@puce.edu.ec (M.A.-M.); nfjativa@puce.edu.ec (N.J.)

[2] International Faculty of Innovation PUCE-Icam, Pontificia Universidad Católica del Ecuador (PUCE), Quito 170143, Ecuador

* Correspondence: jdalbuja@puce.edu.ec

Abstract: The Marchetti Dilatometer test is a non-destructive in situ test that can be used to determine the geotechnical properties of soils. This paper presents the results of a study that investigated the correlations between the parameters obtained from the Marchetti Dilatometer test and geomechanical parameters for soft soils, mainly organic soils, obtained in the laboratory. The study was conducted in the El Garrochal sector in Southern Quito, Ecuador. The results of the study showed that there are significant correlations between the Marchetti Dilatometer test and the undrained shear strength, modulus of elasticity, and density of soil. The equations that were developed in this study can be used to estimate these geomechanical parameters from the results of the Marchetti Dilatometer test for the South Quito sector, which are valuable for geotechnical engineers to design structures in these types of soils. The equations that were developed in this study can be used to improve the accuracy of the design of these structures.

Keywords: Marchetti Dilatometer test; soft soils; organic soils; geomechanical parameters; undrained shear strength; modulus of elasticity; density of soil; correlations

Citation: Mayanquer, J.; Anaguano-Marcillo, M.; Játiva, N.; Albuja-Sánchez, J. New Correlations for the Determination of Undrained Shear, Elastic Modulus, and Bulk Density Based on Dilatometer Tests (DMT) for Organic Soils in the South of Quito, Ecuador. *Appl. Sci.* **2023**, *13*, 8570. https://doi.org/10.3390/app13158570

Academic Editor: Cheng-Yu Ku

Received: 29 June 2023
Revised: 14 July 2023
Accepted: 15 July 2023
Published: 25 July 2023

1. Introduction

A soil study should provide us with reliable geomechanical parameters for analysis of capacity and performance. Many times, the necessary economic resources are not available to perform the variety of tests required to obtain these parameters; therefore, it is decided to estimate them through correlations with information from other tests that are more accessible, quicker, and easier to perform. One of them is the Marchetti Dilatometer, which corresponds to an in situ test; its creator, Silvano Marchetti, provided the engineering community with equations to estimate, by correlation, soil parameters accurately [1]. Although the level of reliability of the correlations is high, they can be complemented with equations applicable to our environment which, in this case, corresponds to soft, mainly organic soils.

The project includes obtaining correlations that allow finding geomechanical parameters of undrained shear strength, modulus of elasticity, and density, in saturated soft soils of the "El Garrochal" sector, using a statistical comparison between the indicators obtained from Marchetti's test (E_D, I_D, and K_D) and geomechanical parameters derived from laboratory tests. To derive equations to obtain, by a correlation between the Marchetti Dilatometer indices and laboratory tests, undrained shear strength, modulus of elasticity, and density parameters that are applicable for use in soil mechanics on soft soils in the "El Garrochal" sector south of Quito, and to complement the Marchetti equations, which have already been published and validated [2,3].

It should be noted that the final product of this work seeks to complement and accompany the correlations that are already in use today and were derived by Marchetti. Since organic soils require an independent study, the results obtained may vary from those obtained by Marchetti's equations. Silvano Marchetti published a series of correlations, which refer to the derivation of soil parameters, based on tests carried out in Italian locations [2]. Although these equations allow us to find reliable geomechanical parameters using the Dilatometer results, and these have been validated in the country, it would be convenient to obtain our equations to increase the level of precision of the parameters to be obtained, especially in organic soils which, due to their composition, require special care at the time of design [4,5].

Relying solely on existing correlations derived from limited geographical locations may not capture the full range of soil behavior and properties. Developing new research on DMT and its correlations enables us to tailor and refine these relationships specifically for different soil types found. This ensures that geotechnical engineers have access to reliable and region-specific correlations, leading to more accurate assessments, optimized designs, and cost-effective solutions for various geotechnical challenges.

The field of site investigation has witnessed a growing trend in the use of in situ tests, driven by recent research papers (e.g., Marchetti 2015 [6], Burlon et al., 2016 [7]). These tests, including the electrical cone penetration test (CPT), piezocone penetration test (CPTu), and the standardized Marchetti flat dilatometer test (DMT), offer rapid, cost-effective, reproducible, and information-rich data [8]. The Marchetti flat dilatometer is particularly valuable as a standardized test that approximates foundation settlement and determines the coefficient K_O of the soil. Ongoing developments have expanded its applications, encompassing controlling compaction systems, identifying sliding surfaces on slopes, evaluating soil liquefaction, assessing deformations in laterally loaded piles, and addressing various geotechnical challenges through correlation-based approaches [9].

Aligned with the concept of spade-shaped in situ testing probes, instrumented DMTs have been developed and examined for diverse objectives [10]. These advancements further enhance the versatility and utility of the flat dilatometer test. The influence of partial drainage is notable, with parameters derived from lift-off pressure significantly affected, while parameters relying on both pressure difference and lift-off pressure show less influence [11]. Despite the benefits of flat dilatometer tests, such as minimal soil disturbance, consistent data, and reliable prediction of in situ soil mechanical properties, challenges arise from factors like pressurization rate, leading to potential errors in test results [12]. Additionally, it is important to note that direct measurement of pore water pressure through flat dilatometer tests is not possible.

Comparisons have been made between the results obtained from the flat dilatometer test and other testing methods, including the standard dilatometer, self-boring pressumeter, seismic cone, and seismic dilatometer. An example of the implementation of new instrumented DMTs is the instrumented flat dilatometer (IDMT) that provides precise and cost-effective measurements of the unload–reload modulus. Furthermore, the comprehensive pressure-displacement curve obtained from the IDMT holds promise for developing improved correlations for strength and initial in situ stresses [13].

The utilization of a multi-parameter/multi-test approach in situ investigation, incorporating tests like CPT, CPTu, and DMT, has gained significant attention as well. Ongoing advancements and research continue to expand the applications of the Marchetti flat dilatometer, while instrumented DMTs offer further possibilities. Although challenges exist in evaluating and correcting errors in flat dilatometer tests, these tests remain valuable in providing crucial insights into soil properties, foundation settlement, and various geotechnical considerations. Exploring these applications further through research allows us to unlock new possibilities and expand the boundaries of geotechnical engineering. By pushing the boundaries of knowledge, we can identify innovative and sustainable solutions to tackle complex geotechnical problems worldwide. In addition, the knowledge of various geomechanical parameters, such as shear strength, stiffness, and deformation characteristics will enhance. This knowledge is crucial for accurate and precise geotechnical analysis and ensures the safety and performance of infrastructure projects.

2. Overview

2.1. Test Site

The location of the study was in Southern Quito, in the “El Garrochal” sector. The boreholes are located at coordinates 0°20′24″ S 78°31′59″ W at an elevation of approximately 2990 m.a.s.l. (Figure 1).

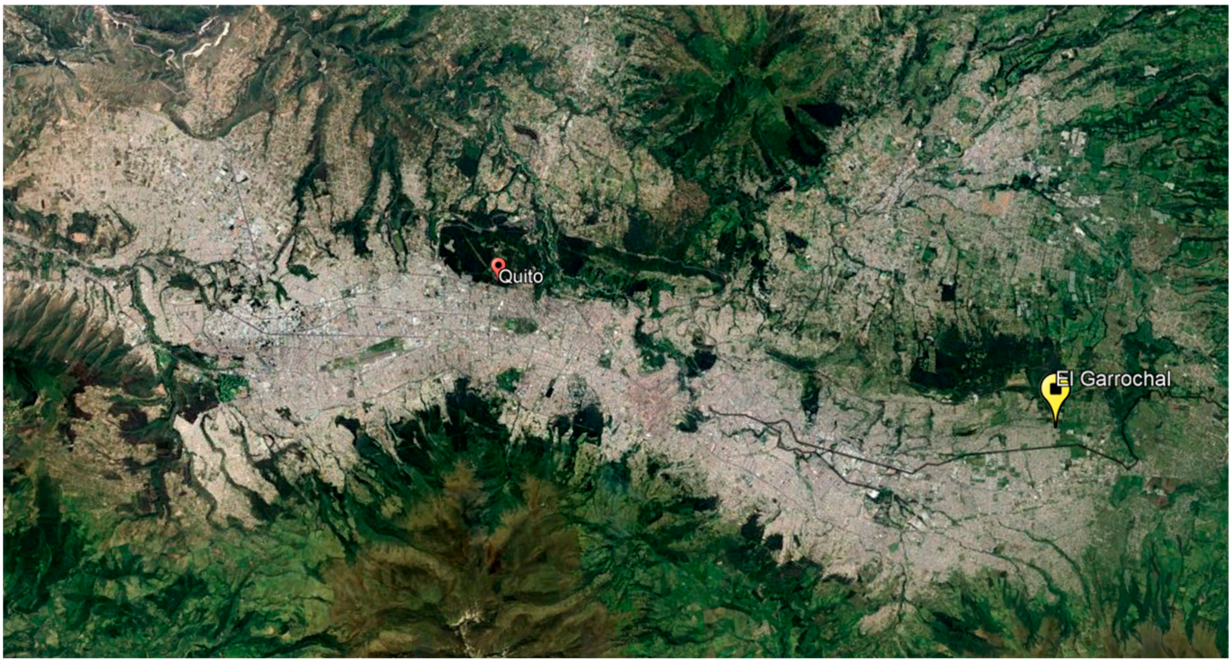

Figure 1. The location where samples were collected.

According to Albuja Sánchez (2018) [3], the “El Garrochal” sector is in the southern valley of Quito. In this valley, there was a lagoon, which drained through the “Machángara” river; however, the lagoon was not completely drained, leaving a superficial water table and organic content, forming a swampy ground. For this reason, according to Santander (2013) [14], the Incas called this sector as “Turubamba”, which is traduced as the Land of Swamps.

A total of 4 boreholes 10 m deep were developed, which were separated with a space of 1.5 m, during the exploration; the water table was located at 1.5 m to 2.00 m from the surface. The ground exploration was developed using a Long Year drilling platform to reach the required depth, as shown in Figure 2a, while to develop the DMT test, the platform presented in Figure 2b was used. A total of 40 samples were extracted according to the ASTM D1587-15 [15]. Nevertheless, a total of 36 samples were used to develop the analysis, due to some tubes presenting with roots, wooden bodies, and mud inside, as seen in Figure 2c,d.

2.2. Laboratory Tests

To develop the research, it was necessary to develop some laboratory tests to obtain the physical and mechanical characteristics of all samples that were analyzed. A summary of laboratory tests was presented in Table 1.

Figure 2. (**a**) Long Year drilling platform, (**b**) DMT platform, (**c**) wooden body found in a Shelby tube, and (**d**) mud found after Shelby's extraction.

Table 1. Summary of laboratory tests.

Laboratory Test	Parameter	Number of Tests	Ref.
Moisture content	W (%)	36	[16]
Atterberg Limits	LL, LP, IP (%)	36	[17]
Material finer than 75 µm	%Fines	36	[18]
USCS Classification	Soil Classification	36	[19]
Ash and organic content	Ash content, Organic material	36	[20]
Density (Unit weight) of soil	γ, ρ	35	[21]
Triaxial UU	C_u, E	31	[22]

Specimen Preparation

The laboratory tests were performed in the Laboratory of Material Resistance, Soil Mechanics, Pavements and Geotechnics of Pontifical Catholic University of Ecuador. As mentioned in Section 2.1, the Shelby tubes were extracted by [15], covered with plastic to conserve the moisture content, and stored in a room without sun light, as seen in Figure 3a. Subsequently, to perform the laboratory tests, the Shelby tube samples were extracted (Figure 3b), photographed (Figure 3c), and stored with their corresponding identification (Figure 3d) and analyzed according to the tests presented in Table 1.

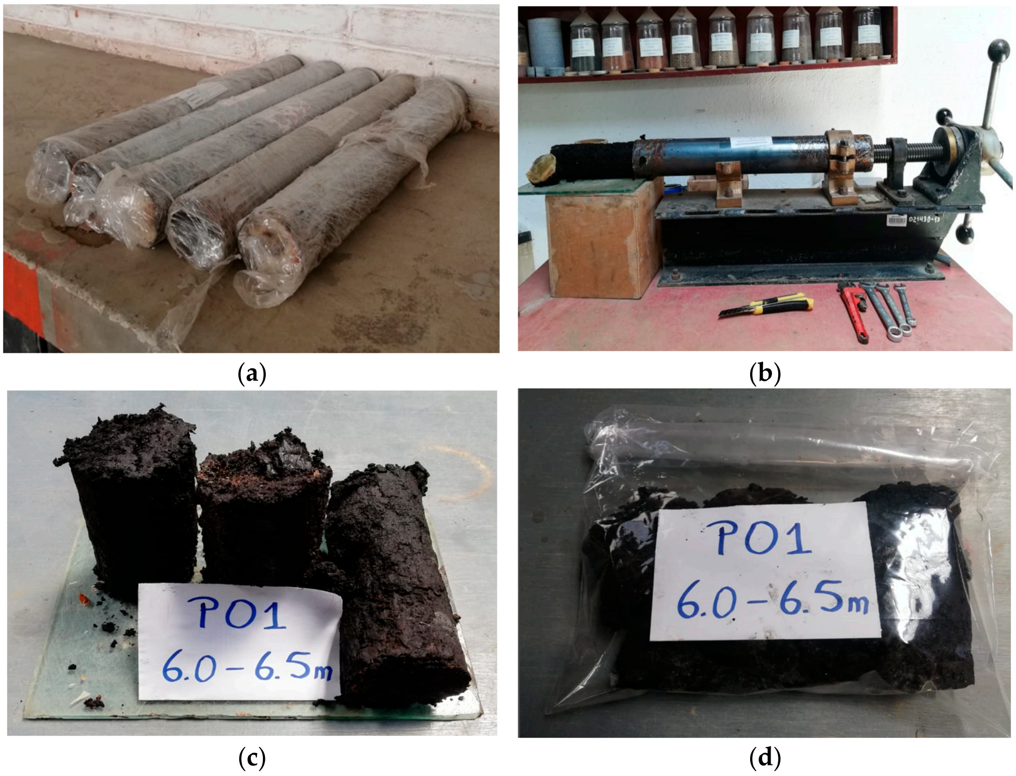

Figure 3. (**a**) Extracted Shelby tubes, (**b**) sample being extracted from a Shelby tube, (**c**) photographed samples, and (**d**) stored samples.

Four Shelby tube samples were extracted per week for the execution of the laboratory tests, with the objective of advancing the investigation.

2.3. Marchetti Dilatometer: Conceptualization

The Dilatometer is an in situ penetration and expansion test proposed by Silvano Marchetti in 1980, which consists of the insertion of a stainless-steel sheet at intervals. This stainless-steel sheet has a membrane on one side, which is inflated by a pressurized gas injected through a system of tubes.

This test measures the horizontal stress that must be recorded at certain points of the operation called pressure values A and B [23], as shown in Figure 4. The procedure to obtain these values is standardized by the ASTM D6635-15 [24] and Marchetti in its publications. The present research used the procedures and equations proposed by [24], and Marchetti's procedure and equations for obtaining indexes, which are present in [23], where Marchetti proposed the concept of the Dilatometer to the engineering community; however, these are no longer used or recognized for research use.

Marchetti presented a series of correlations as part of his study in 1980. These covered the OCR, K_o, C_u, and the edometric modulus value through the trend of these values about the I_D, E_D, and K_D indexes [23]. Nowadays, the researchers have the following equations, presented in Table 2, published in 2001 by the International Society for Soil Mechanics and Geotechnical Engineering [2].

Table 2 showed that the undrained shear strength equation involved the value of K_D and the effective vertical stress. It was also restricted by the material index (I_D), which can be identified as clay ($0.1 < I_D < 0.6$), silt ($0.6 < I_D < 1.8$), and sand ($1.8 < I_D < 10$) [2]. Based on this, this restriction corresponded to silts and clays, due to $I_D < 1.2$. However, [2,24] reports recommended that this equation only be used on clays, which limits its use in soil volumes where silts predominate [2,24].

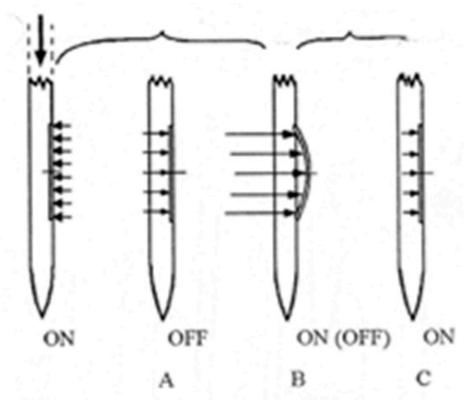

Figure 4. Basic principles of Marchetti Dilatometer: pushing, contact stress A, expansion stress B, pressure C, adapted from [4].

Table 2. Basic DMT reduction formulae, Marchetti (2001) [2].

K_o	[-]	Coeff. Earth Pressure	$K_{o,\ DMT} = (K_D/1.5)^{0.47} - 0.6$	For $I_D < 1.2$
OCR	[-]	Overconsolidation Ratio	$OCR_{DMT} = (0.5 * K_D)^{1.56}$	For $I_D < 1.2$
C_u	[kPa]	Undrained Shear Strength	$C_{u,\ DMT} = 0.22 * \sigma'_{vo} * (0.5 * K_D)^{1.25}$	For $I_D < 1.2$
$\varnothing$	[°]	Friction Angle	$\varnothing_{safe,\ DMT} =$ $28^\circ + 14.6^\circ * \log(K_D) - 2.1^\circ \log^2(K_D)$	For $I_D > 1.8$
C_h	[cm^2/min]	Coefficient of consolidation	$C_{h,\ DMTA} \approx 7\ \text{cm}^2/t_{flex}$	t_{flex} from along A-log t DMT-A decay curve
k_h	[cm/min]	Coefficient of permeability	$k_h = C_h * \gamma_w / M_h \quad ; \quad M_h \approx K_o * M_{DMT}$	-
γ	[kN/m^3]	Unit Weight and Description	(See Figure 5, considering $\gamma_w = 9.81$ kN/m^3).	-
M	[MPa]	Vertical Drained Constrained Modulus	$M_{DMT} = R_M * E_D$ If $I_D \leq 0.6$ $R_M = 0.14 + 2.36 * logK_D$ If $I_D \geq 3$ $R_M = 0.5 + 2 * logK_D$ If $0.6 < I_D < 3$ $R_M = R_{M,0} + (2.5 - R_{M,0}) * logK_D$ $R_{M,0} = 0.14 + 0.15 * (I_D - 0.6)$ If $K_D > 10$ $R_M = 0.32 + 2.18 * logK_D$ If $R_M < 0.85$, set $R_M = 0.85$	-

As for the modulus of elasticity, it should be noted that it is obtained through the edometric modulus value. The standard provides expressions to calculate this parameter considering different limitations to find the correction factor R_M. These limitations are given by the values of I_D, K_D, and R_M, as shown in Table 2. The product between R_M and E_D is the value of the dilatometer modulus.

According to Rabarijoely (2018) [4], the nomogram chart developed by Larsson (1989) [25], is a graphical tool that can be used to determine the type of soil and its bulk density, which is based on two values on the adjusted value of the material index, $I_{D(kor)}$, and the dilatometer modulus, E_D. To obtain the density, there is no defined equation; however, this nomogram helps to obtain this parameter. Figure 5 presents how it relates the values of E_D with those of I_D—in this way, the intersection of these data marks the value of the ratio of the unit weight of soil to the unit weight of water (γ_s/γ_w), in addition to allowing the classification of the material.

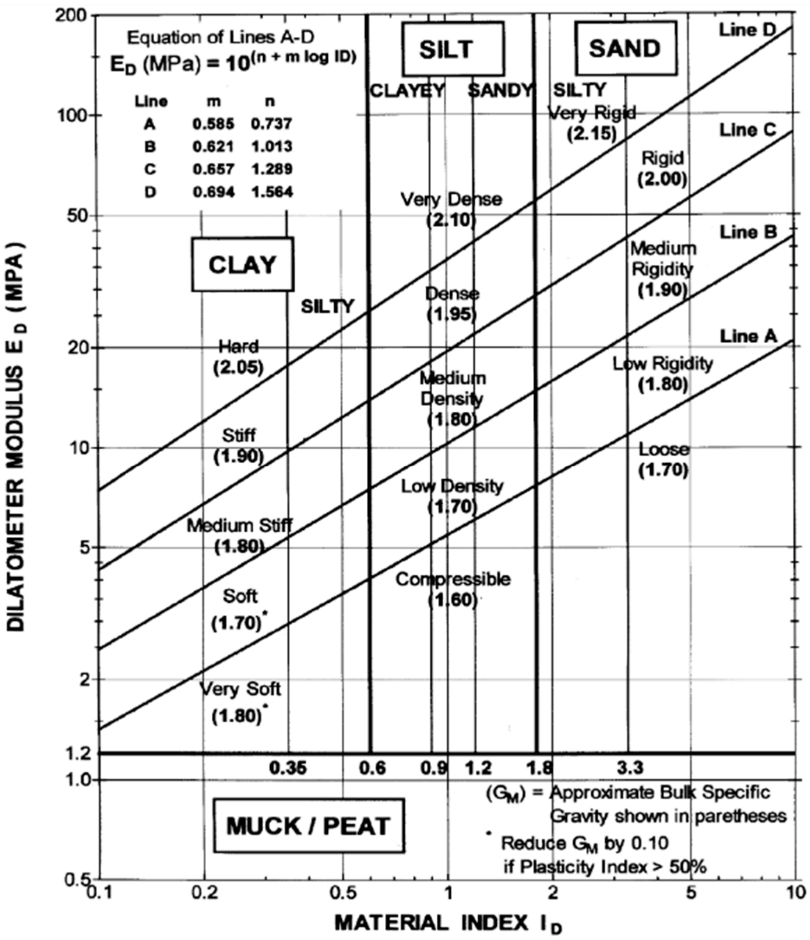

Figure 5. Marchetti's nomogram for estimating soil type and unit weight γ, [26].

3. Results

3.1. Laboratory Tests Results

3.1.1. Atterberg Limits

The results obtained from the Atterberg Limits Test are presented in Figure 6, in which the 94.44% of the data plots above an LL equal to 50 and below the A-line, corresponding to a high-plasticity type of plasticity.

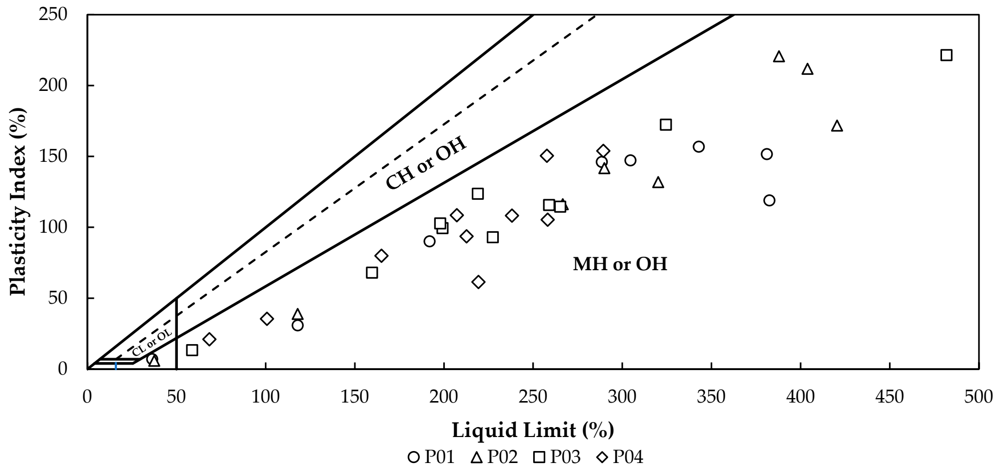

Figure 6. Plasticity chart with results of each borehole.

To define the type of material, which can be inorganic or organic silt, a verification of LL was done. It consisted of determining the LL in several blows of 25 ± 1 with oven-dried material. If the ratio of the $LL_{\text{oven dried}}$, with respect to the $LL_{\text{not dried}}$, is lower than 0.75, it was classified as organic [19]. Furthermore, to show how the behaviors of the LL and IP are with respect to deep, Figure 7 is presented below.

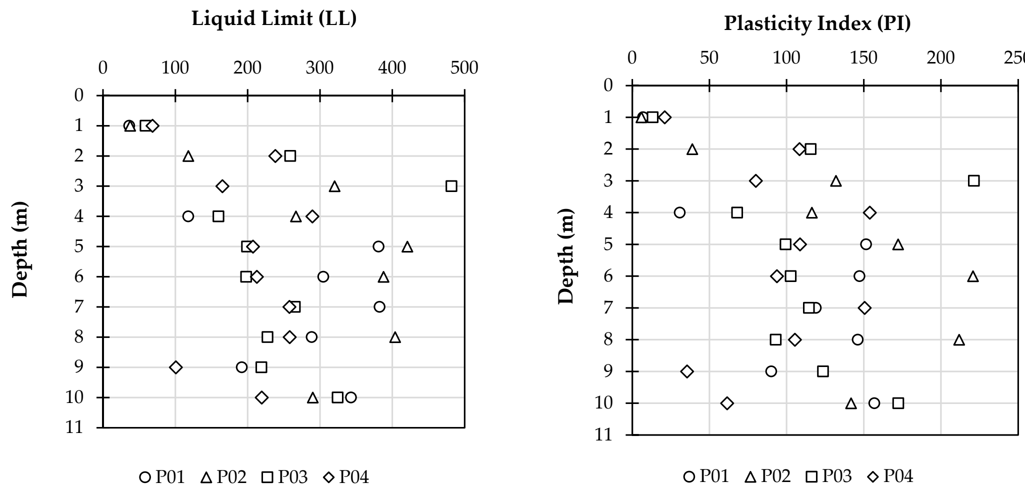

(**a**) (**b**)

Figure 7. (**a**) Variation of the LL, with respect to depth; (**b**) variation of PI, with respect to depth.

3.1.2. Granulometry

All samples were tested using the ASTM D1140 [18]. Nevertheless, the results showed that the greatest amount of material passed through the N°200 sieve (75 μm)—see Figure 8—leaving a very little amount of material retained in the rest of the sieves (N°4, 10, 40), with an aperture size bigger than 75 μm. In Figure 9, it was noted that the part that was retained corresponded to the organic content composed of roots and organic material.

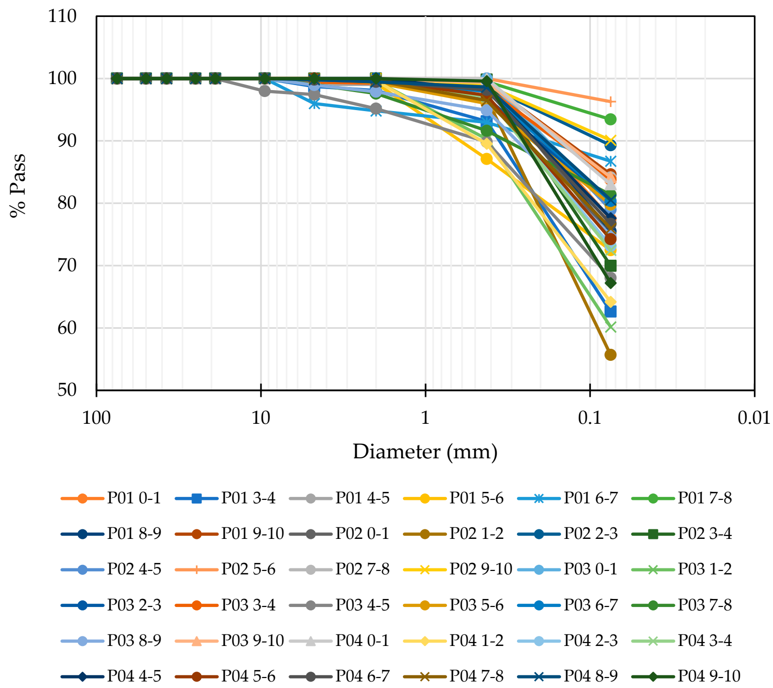

Figure 8. Particle size distribution of samples of all boreholes.

(a) (b)

Figure 9. (**a**) Organic material retained above the N°200 sieve; (**b**) fine sand retained above the N°200 sieve.

3.1.3. Ash and Organic Content

To know the amount of organic matter present in a sample, it is necessary to determine the percentage of dry weight remaining after having submitted it to an incineration process—this value is better known as ash content. The difference in this percentage—about 100%—is the organic content present in the sample [27,28].

As shown in Figure 10, the results of ash content have a very well-marked tendency, as the values oscillate between 60% and 90%. Furthermore, Sutejo et al. (2017) [29], related to the classification of peat, provides a classification of the material according to its ash content (Table 3). In addition, the ASTM D653-22 [30] mentions that to distinguish peat from organic soil, it must have less than 25% ash content by dry weight; therefore, the tabulated results corresponded to organic soils with a high ash content and an organic content ranging from 0% to 40%.

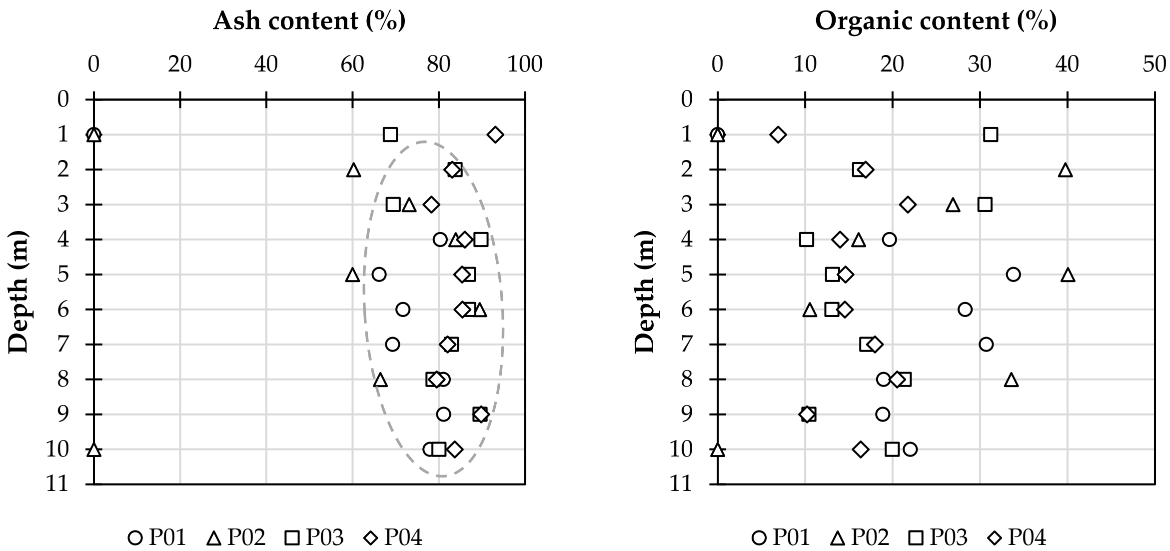

(a) (b)

Figure 10. Variation of (**a**) ash content and (**b**) organic content of each borehole about depth.

Table 3. Soil classification according to ash content, [29].

Ash Content	Description
Low ash	<5% ash
Medium ash	5–15% ash
High ash	>15% ash

3.1.4. Summary of Laboratory Tests Results

This section presents a summary of the results obtained from laboratory tests for each borehole per meter of drilling in Tables 4–7.

Table 4. Summary of results for the first borehole.

Depth (m)	Moisture (%)	LL (%)	PL (%)	PI (%)	Organic	Ash Content	Organic Content	Soil Type
0–1	40.74	36.37	29.35	7.02	No	0	0	ML, Silt with Sand
1–2	-	-	-	-	NA	-	-	NA
2–3	-	-	-	-	NA	-	-	NA
3–4	276.38	117.98	87.17	30.81	Yes	80.35	19.65	OH, Organic Sandy Silt
4–5	527.32	381.09	229.54	151.55	Yes	66.17	33.83	OH, Organic Sandy Silt
5–6	554.39	304.63	157.42	147.21	Yes	71.70	28.30	OH, Organic Sandy Silt
6–7	520.98	382.52	263.59	118.93	Yes	69.28	30.72	OH, Organic Silt
7–8	223.88	288.55	142.45	146.10	Yes	81.03	18.97	OH, Organic Silt
8–9	195.91	191.94	101.88	90.06	Yes	81.12	18.88	OH, Organic Sandy Silt
9-10	499.98	342.92	186.07	156.85	Yes	77.96	22.04	OH, Organic Sandy Silt

Table 5. Summary of results for the second borehole.

Depth (m)	Moisture (%)	LL	PL	PI	Organic	Ash Content	Organic Content	Soil Type
0–1	39.15	37.52	31.63	5.89	No	0	0	ML, Silt with Sand
1–2	274.39	117.94	79.07	38.87	Yes	60.24	39.76	OH, Organic Sandy Silt
2–3	335.72	320.19	188.22	131.97	Yes	73.10	26.90	OH, Organic Sandy Silt
3–4	388.33	266.67	150.30	116.37	Yes	83.89	16.11	OH, Organic Sandy Silt
4–5	489.88	420.82	248.61	172.21	Yes	59.96	40.04	OH, Organic Sandy Silt
5–6	374.55	387.87	167.12	220.75	Yes	89.47	10.53	OH, Organic Silt
6–7	-	-	-	-	NA	-	-	NA
7–8	485.71	403.80	192.03	211.77	Yes	66.42	33.58	OH, Organic Sandy Silt
8–9	-	-	-	-	NA	-	-	NA
9–10	305.18	289.92	148.19	141.73	Yes	0	0	OH, Organic Sandy Silt

Table 6. Summary of results for the third borehole.

Depth (m)	Moisture (%)	LL	PL	PI	Organic	Ash Content	Organic Content	Soil Type
0–1	109.39	58.85	45.59	13.26	Yes	68.77	31.23	OH, Organic Sandy Silt
1–2	288.30	258.95	143.32	115.63	Yes	83.77	16.23	OH, Organic Sandy Silt
2–3	493.22	481.83	260.43	221.40	Yes	69.42	30.58	OH, Organic Sandy Silt
3–4	178.36	159.70	91.70	68.00	Yes	89.81	10.19	OH, Organic Sandy Silt
4–5	260.82	199.20	99.80	99.40	Yes	86.85	13.15	OH, Organic Sandy Silt
5–6	243.07	197.95	95.25	102.70	Yes	86.92	13.08	OH, Organic Sandy Silt
6–7	299.12	265.21	150.70	114.51	Yes	82.94	17.06	OH, Organic Sandy Silt
7–8	266.08	227.43	134.46	92.97	Yes	78.66	21.34	OH, Organic Sandy Silt
8–9	212.11	219.09	95.47	123.62	Yes	89.56	10.44	OH, Organic Sandy Silt
9–10	299.22	324.52	152.17	172.35	Yes	80.04	19.96	OH, Organic Sandy Silt

Table 7. Summary of results for the fourth borehole.

Depth (m)	Moisture (%)	LL	PL	PI	Organic	Ash Content	Organic Content	Soil Type
0–1	60.66	68.45	47.38	21.07	Yes	93.09	6.91	OH, Organic Sandy Silt
1–2	264.02	238.17	129.85	108.32	Yes	83.08	16.92	OH, Organic Sandy Silt
2–3	351.01	164.97	84.94	80.03	Yes	78.26	21.74	OH, Organic Sandy Silt
3–4	207.70	289.37	135.46	153.91	Yes	86.01	13.99	OH, Organic Sandy Silt
4–5	240.76	207.29	98.65	108.64	Yes	85.39	14.61	OH, Organic Sandy Silt
5–6	257.50	212.69	118.99	93.7	Yes	85.47	14.53	OH, Organic Sandy Silt
6–7	346.91	257.74	107.2	150.54	Yes	82.02	17.98	OH, Organic Sandy Silt
7–8	249.88	258.11	152.72	105.39	Yes	79.49	20.51	OH, Organic Sandy Silt
8–9	129.01	100.74	65.26	35.48	Yes	89.78	10.22	OH, Organic Sandy Silt
9–10	282.83	219.32	157.88	61.44	Yes	83.66	16.34	OH, Organic Sandy Silt

3.1.5. Density (Unit Weight) of Soil

To find the density values, the samples were subjected to the process described in [21]. It consisted of determining the density of soil by immersing it and calculating the difference in volume which was displaced. However, during the tests, it was found that, in certain cases, the material turned out to be lighter than water, and this did not allow the paraffin-coated samples to be immersed in the container with water. To solve this problem, it was decided to change the liquid in which the samples were immersed, this had to be less dense than water, so commercial Diesel with a density of 0.84 g/cm^3 was used; in this way, it was possible to verify that in this type of soil, it was preferable to use fluids with these characteristics to avoid flotation. A summary of the results is presented in Figure 11.

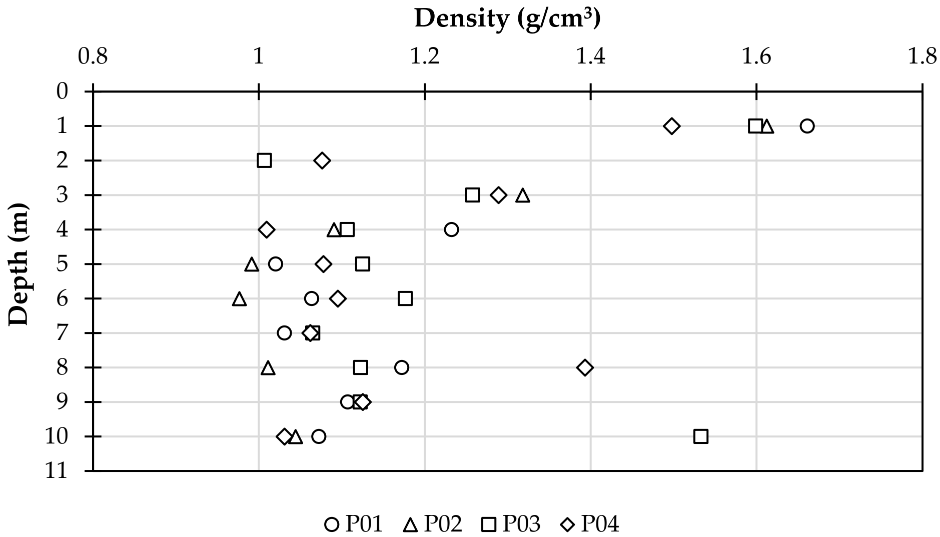

Figure 11. Variation of density values of each borehole about depth.

3.1.6. Relative Density

The type of soil is important for determining the best method for calculating the degree of compaction (Dr) and the degree of saturation (S). Therefore, it is important to become familiar with the conditions of the study area, such as the geology, stratigraphy, and hydrology [31]. Although consideration was given to finding the specific gravity of the recovered samples, several mishaps made this task so difficult that it could not be performed in the laboratory. In the first place, the scarcity of material required that it be prioritized in the most important tests. In addition, the material, due to its consistency, when submerged in the pycnometers, would have remained suspended without settling on the base, which would lead to erroneous results. It was advisable to find the specific gravity of the organic content and similar separately since these were the ones that tended to be lighter than water, and to use pycnometers with an automatic helium gas injection to obtain more accurate results [3].

Despite the above, it was decided to use the following Equation (1) to obtain the specific gravity values for our material using its ash content [32].

$$G = \frac{(2.7 * 1.4)}{(2.7 - 1.4) * \left(1.04 * \frac{N}{100} - 0.04\right) + 1.4} \quad (1)$$

where:

G: specific gravity.

N: ignition loss (%).

Figure 12 shows that the specific gravity of soils ranges between 1.45 and 1.75. These values were validated with the research developed by Li et al. (2020) [33], using the following expression:

$$G_s = \frac{3.74}{N * 1.42 + 1.35} \quad (2)$$

where:

G_s: specific gravity.

N: ignition loss (%).

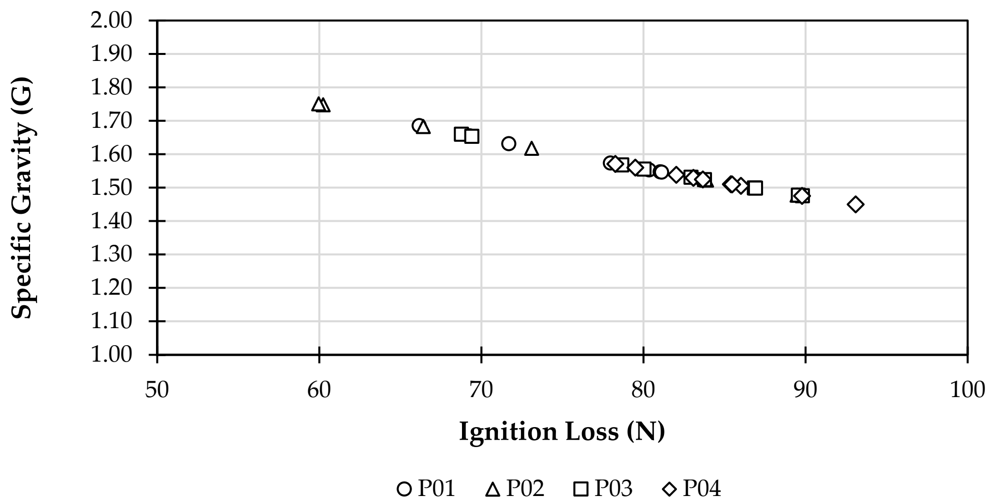

Figure 12. Relationship between the specific gravity of the soil and its ash content, using equation 1.

Figure 13 shows that the specific gravity of soils ranges between 1.40 and 1.70.

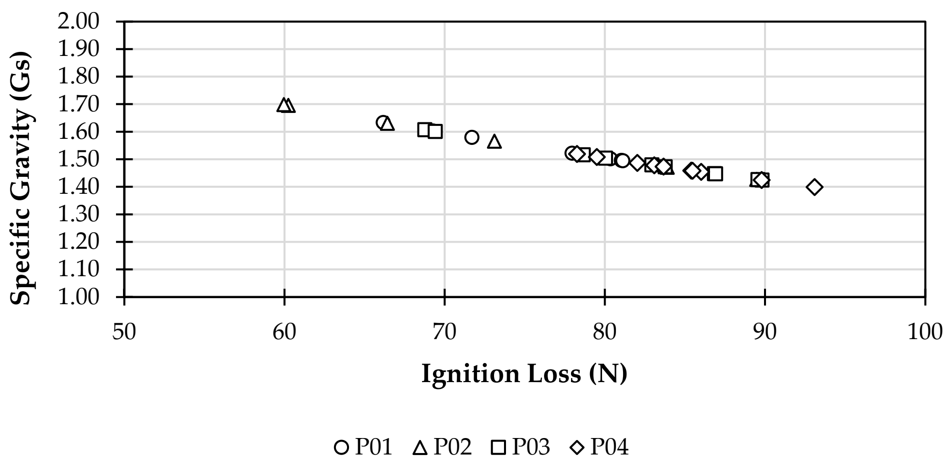

Figure 13. Relationship between the specific gravity of the soil and its ash content, using equation 2.

3.1.7. Triaxial UU

The undrained, unconsolidated triaxial tests were performed in saturated specimens and tested according to the ASTM D2850 [22]. The saturation of these samples was controlled before their compression with the Skempton value "B", which must be greater than 0.95 to consider that one sample is saturated [34]. In addition, to define the confinement applied to the specimens, the results presented in Figure 11 were used, because according to [34] it was appropriate to use the effective in situ stress in the first specimen and the following samples must have been confined using a double stress of the sample tested before.

The ASTM D2850 mentions that to develop this test, three specimens should be used, and if necessary, at least two to obtain a correct analysis of results [22]. However, given the lack of material or that it was not suitable to be molded (Figure 14), certain tests were performed using only one specimen.

Figure 14. Samples that were not suitable to be molded.

However, soft soils, such as clay, when subjected to the Triaxial UU test tend to present a completely horizontal Mohr–Coulomb envelope, which means that the soil is purely cohesive since the friction angle is equal to 0. It occurs because the material does not drain, and therefore, the applied load is supported only by the water pressure in the pores [22]. Consequently, considering this behavior, in particular cases, just one specimen was tested and used the value of the radius to obtain the undrained shear strength (C_u). The results of C_u are presented in Figure 15a.

Elasticity modulus in soils is one of the most difficult parameters to determine; different authors state that its calculation is based merely on predictions using the materials theory. For this reason, there are several methods to find it: initial tangent, secant, recharge, discharge, and cyclic; each of these is based on drawing a line on the curve and calculating the slope of this to find the modulus [35]. The initial tangent model was used since it was commonly used to represent the modulus of undrained soil due to the elastic response that was evident near the origin of the curve. Nevertheless, this does not mean that it was the optimal model when determining this parameter [36]. The results of the elasticity modulus are presented in Figure 15b.

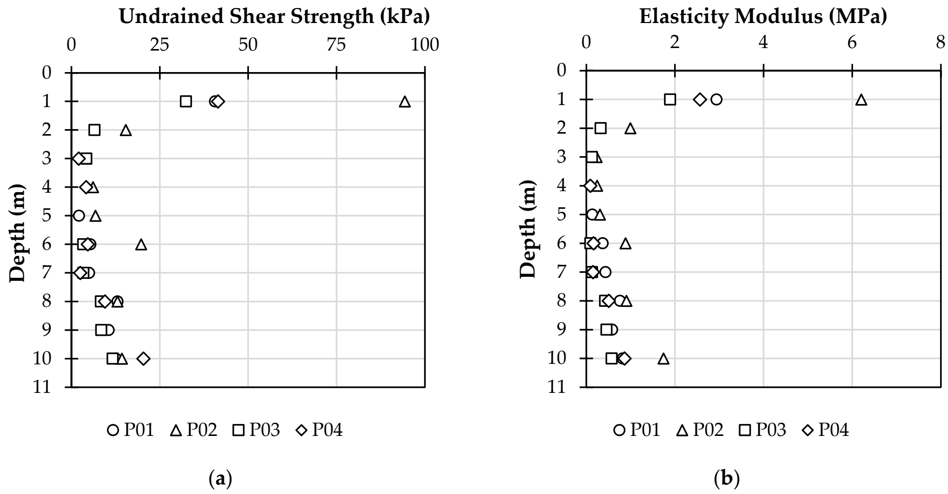

Figure 15. (**a**) Variation of C_u and (**b**) the elasticity modulus of each borehole about depth.

3.2. Dilatometer Results

The execution of the dilatometer test was carried out in the same location as the drilling boreholes for the extraction of samples. The necessary calibration was performed before the insertion of the apparatus into the soil in each borehole. The corresponding results of I_D, K_D, and E_D for each borehole are presented in Figure 16.

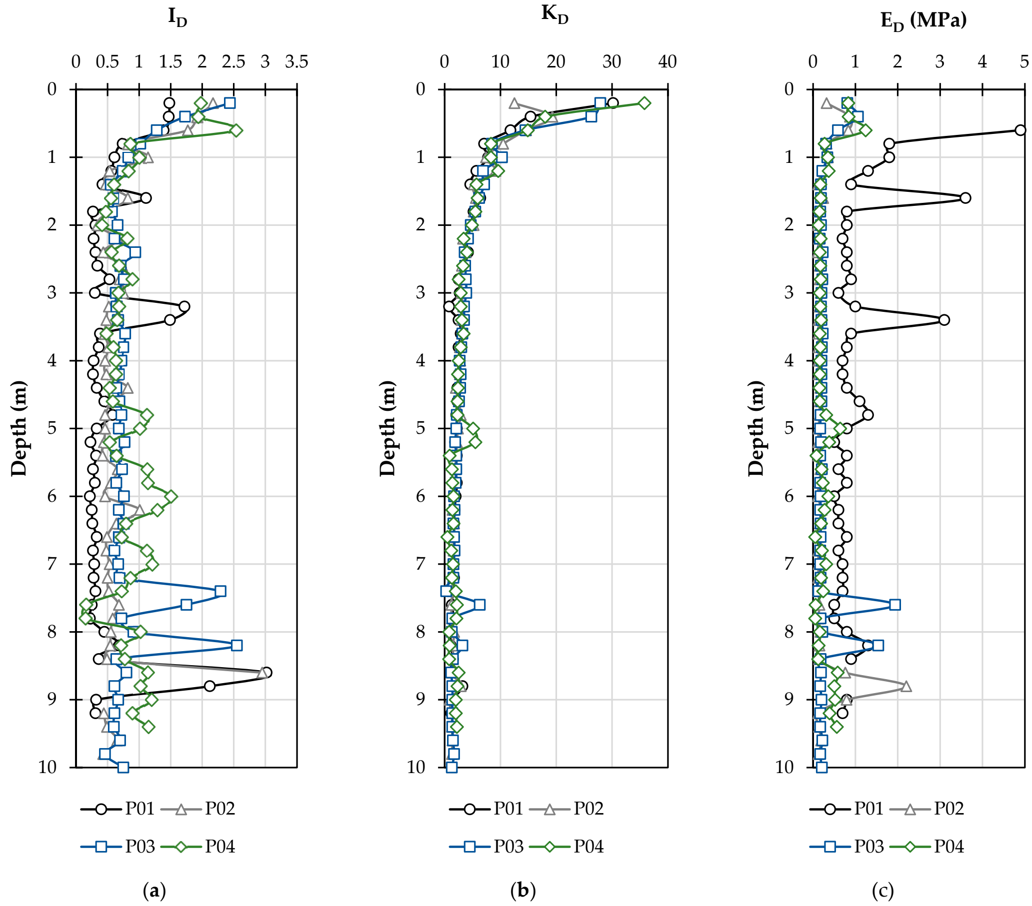

Figure 16. Variation of (**a**) material index (I_D), (**b**) horizontal stress index (K_D), and (**c**) dilatometer modulus (E_D) of each borehole about depth.

The data were compiled from the report generated by the DMT software. The results that were obtained coincided with the expected values for organic soils, because the soils that had E_D values that were less than or equal to 12 bars (1.2 MPa) would be considered organic or peaty (MUCK/PEAT) [2]. Furthermore, Albuja-Sánchez (2018) [3], in his research, collected DMT data in the "Turubamba" sector, which also presented the same type of material as in this study.

Figure 17 is presented as Marchetti's nomogram with the results that were obtained from the DMT test, in which it can be observed that most of data were plotted in the MUCK/PEAT nomogram's sector. In addition, the value of relation, γ_s/γ_w, can be determined to obtain the unit weight of soil.

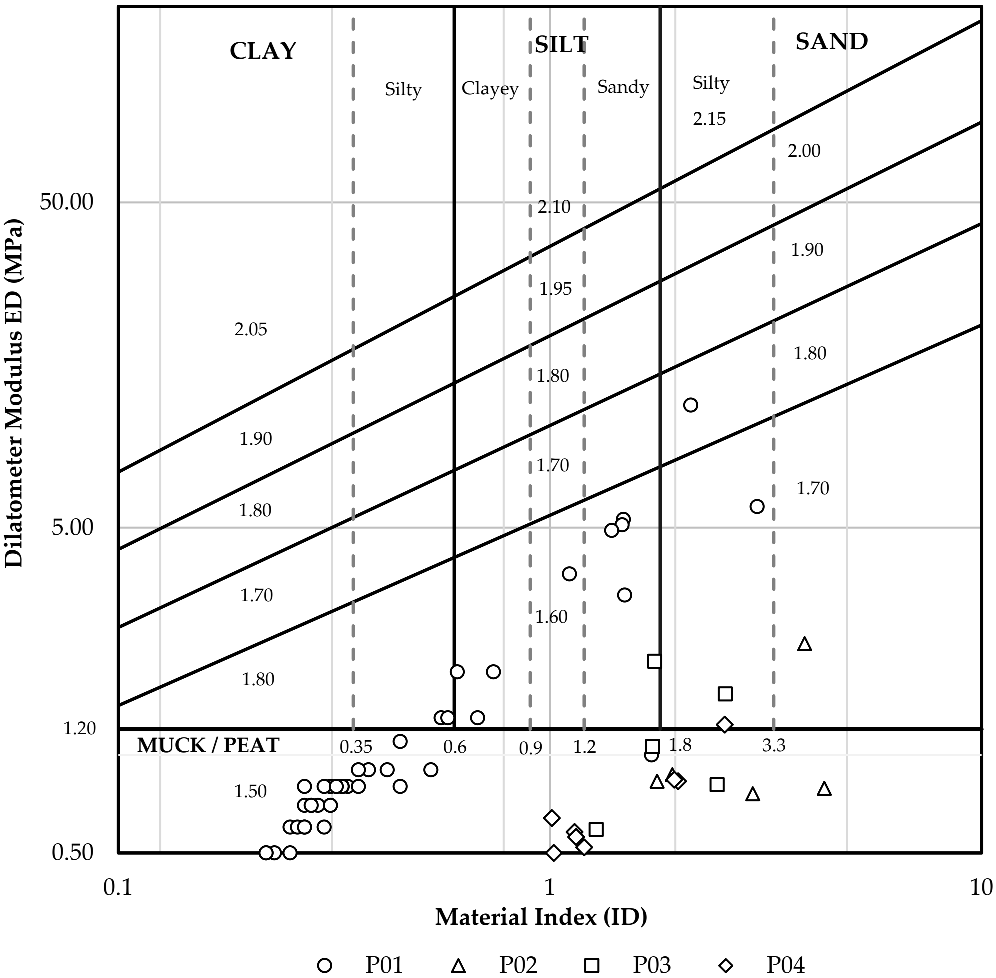

Figure 17. Results of the DMT plotted on Marchetti's nomogram.

4. Discussion

Based on the DMT test indexes and geomechanical parameters obtained from laboratory tests, three equations were found that will allow us to find values for the modulus of elasticity, undrained cohesion, and density in organic soils. The values obtained from the laboratory were compared with the values calculated with the Marchetti equations.

4.1. Elasticity Modulus (E)

The modulus of elasticity equation was proposed and validated by Marchetti, relating to the value of E_D, to the value of the modulus of elasticity itself, and is limited by the value of I_D and K_D [24]. However, according to [2], the value of the elasticity modulus cannot be directly equal to E_D due to the absence of information about the stresses that soil has undergone in its history. Hence, the elasticity modulus was approximately 80% of the edometric modulus or M_{DMT}.

To find a correlation between the elasticity modulus (E) and the dilatometer modulus (E_D), it was necessary to see how the behavior of E about I_D was (Figure 18), because the material index (I_D) was used to define the type of material.

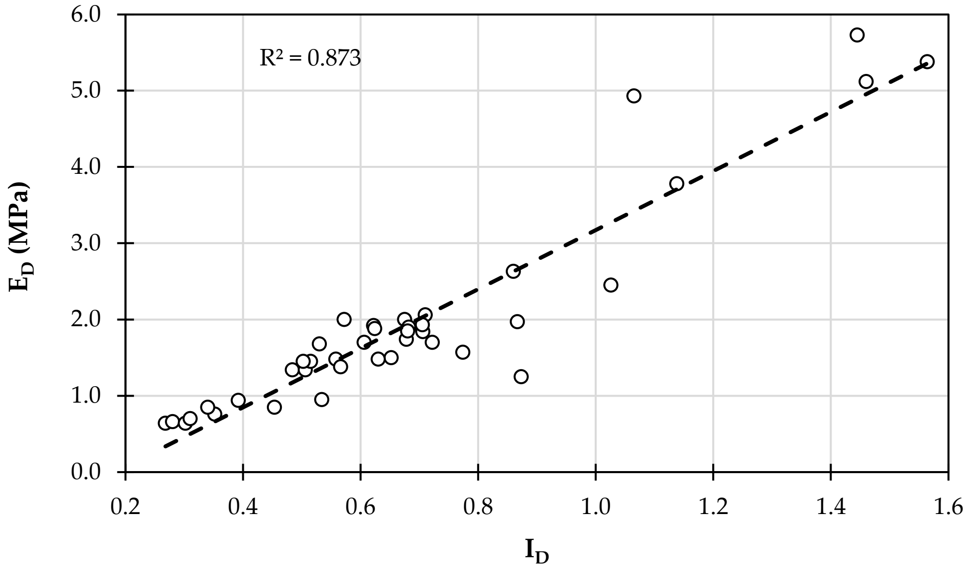

Figure 18. Relationship between the I_D and E_D of all collected data.

Figure 18 presented that the dilatometer modulus (E_D) was proportional directly to I_D, presenting a lineal relationship, with R^2 equal to 0.873. Moreover, 85% of I_D values were less than 1, so the equation presented in Figure 19 has a higher degree of effectiveness for soils with an I_D of less than 1.

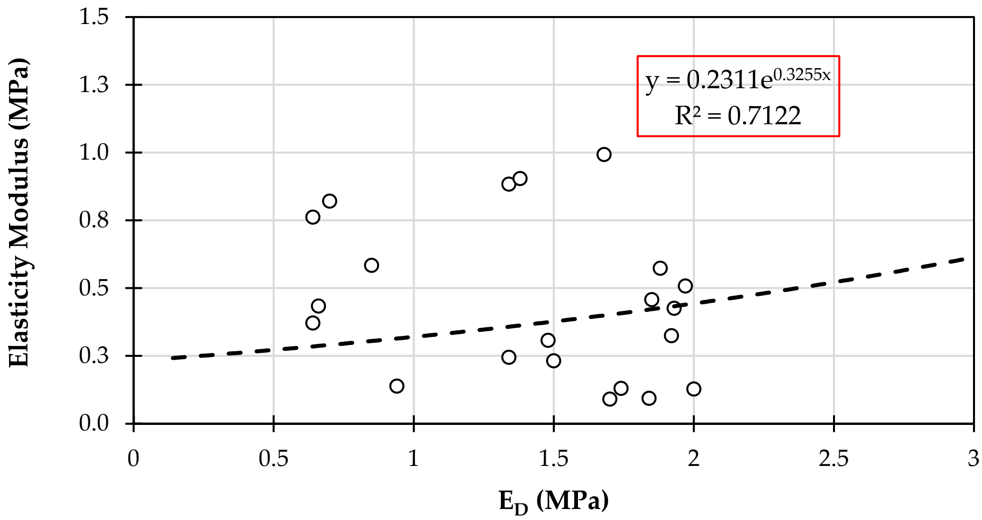

Figure 19. Correlation and regression equation to obtain the modulus of elasticity.

Figure 20 shows that the modulus of elasticity results obtained in the laboratory decrease with an increasing depth, presenting a potential tendency with an R^2 equal to 0.4881.

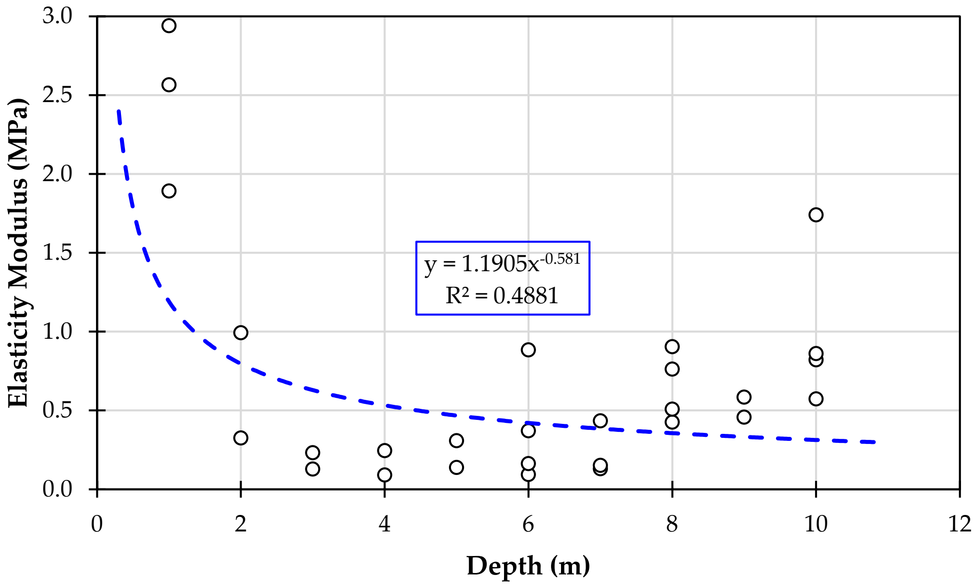

Figure 20. Correlation equation based on test results and depth for modulus of elasticity.

A comparison was also presented between the results obtained using the equations currently in force based on Marchetti's studies and the data obtained in the laboratory, which is presented in Figure 21.

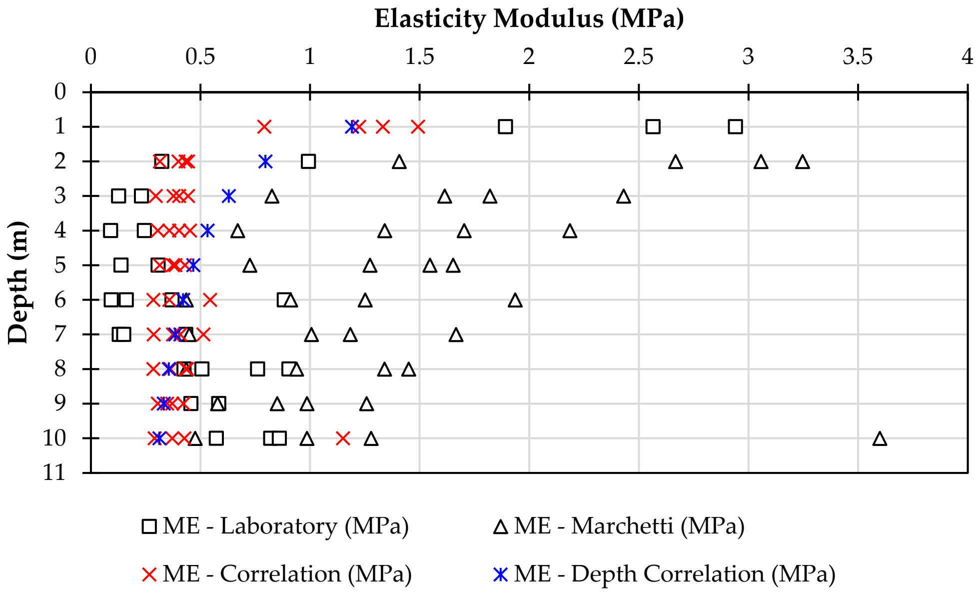

Figure 21. Comparison between different elasticity modulus values.

Figure 21 showed that Equation (3) had the best fit, with respect to the expected results, which ranged between 0.2 MPa and 0.5 MPa. Therefore, an exponential model (Figure 19) was chosen to obtain consistent values of the elasticity modulus considering the real data. Nevertheless, considering that the E_D depended directly on the I_D (Figure 17), Equation (3) was limited to I_D values less or equal to 1.

$$E = 0.231e^{0.326E_D}, \quad I_D \leq 1 \tag{3}$$

The results of Equation (3), which were presented in Figure 19, show the variation between the three values of elasticity modulus. The data presented by Marchetti presented extremely high values concerning the values obtained in the laboratory tests. Equation (3) derived in this work, although it provided low results for more consistent materials, presenting a trend with more accurate values for organic soils with a low I_D equal to or less than 1.

In addition, it was possible to observe that the trend generated from the laboratory results and depth (Equation (4)) presented higher values than those obtained in Equation (3) in meters 2 and 3. However, from meter 4 to meter 10, it adapted better to the results obtained by the equation as a function of E_D, as shown in Figure 21.

$$E = 1.191z^{-0.581} \tag{4}$$

where:

z: depth, m.

4.2. Undrained Shear Strength (C_u)

To develop this study, the Equation (5), proposed by Marchetti, was used to start the analysis, because it related the undrained shear strength with the vertical effective stress and the K_D, considering that the I_D must be less than 1.2.

$$C_u = 0.22\sigma'_{vo}(0.5K_D)^{1.25},\ I_D < 1.2 \tag{5}$$

In this way, the following parametric Equation (6) was used to determine the appropriate regression:

$$C_u = A * \sigma'_{vo}(B * K_D)^C,\ I_D < 1.2 \tag{6}$$

In Figure 22, it should be noted that the data found were scattered among themselves. However, a trend was found between meter 2 and meter 10. Consequently, the regression was performed based on the data corresponding to meter 2 and meter 10. In addition, these data provide consistent values of undrained shear strength for the type of soil that was relevant to this study.

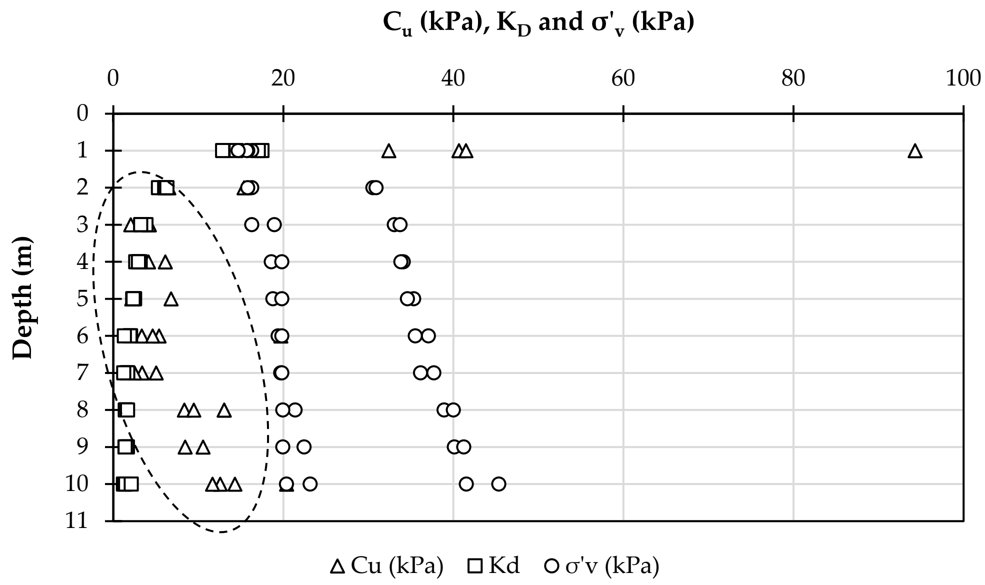

Figure 22. Undrained shear distribution, K_D, and vertical effective stress about depth.

Furthermore, as shown in Figure 22, the zone marked between meters 2 and 10, C_u and K_D had values that were close to each other. It must be considered that the C_u value had a directly proportional relationship with depth. Therefore, the equation to be obtained must consider this effect. Using the Minitab program, the correlation coefficients between variables and the regression that provided the equation for the calculation of the undrained shear strength were obtained.

Figure 23 shows the relationship between each variable. According to Hernández, Fernandez, and Baptista (2014) [37], the K_D and C_u, as well as the σ'_v and K_D, were inversely proportional; whereas, C_u and σ'_v were directly proportional. Hence, an equation was obtained based on the structure proposed by Marchetti (Equation (6)) and using the data between meter 2 and meter 10, the equation is presented below.

$$C_u = 0.262\sigma'_{\mathrm{vo}} K_D{}^{-0.221},\ I_D \leq 1 \quad (7)$$

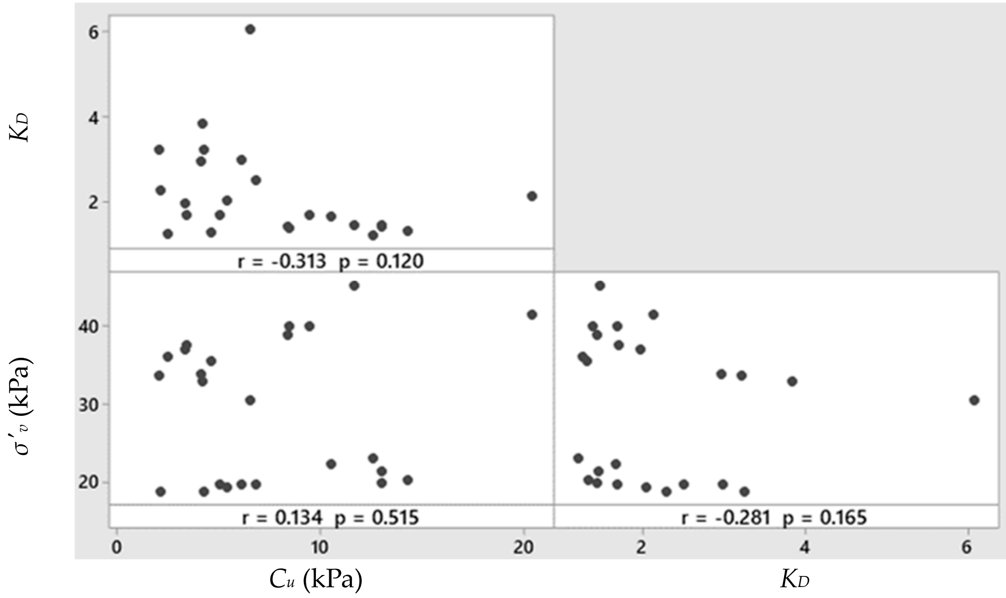

Figure 23. Relationship between variables (C_u, K_D, and σ'_v).

Figure 24 shows that the undrained shear strength results obtained in the laboratory decrease with increasing depth, presenting a potential tendency with an R^2 equal to 0.4784.

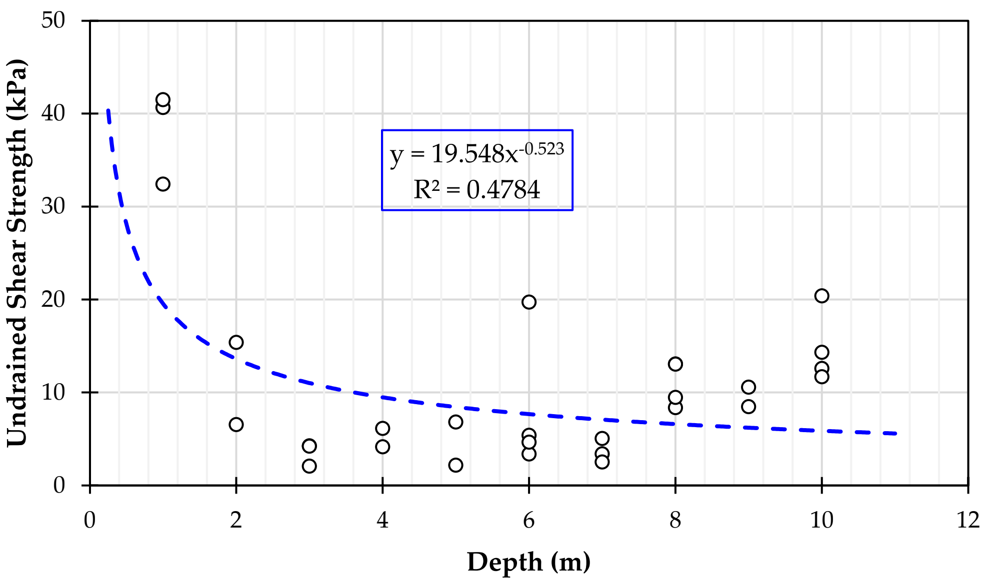

Figure 24. Correlation equation based on test results and depth for undrained shear strength.

This equation was useful to obtain the undrained shear strength of very soft soils, such as organic soils. Therefore, it was limited by I_D values less than 1. With the previous equation, Figure 25 shows that the undrained shear strength values were close to those found by laboratory tests; however, these differ from those obtained using the Marchetti equation.

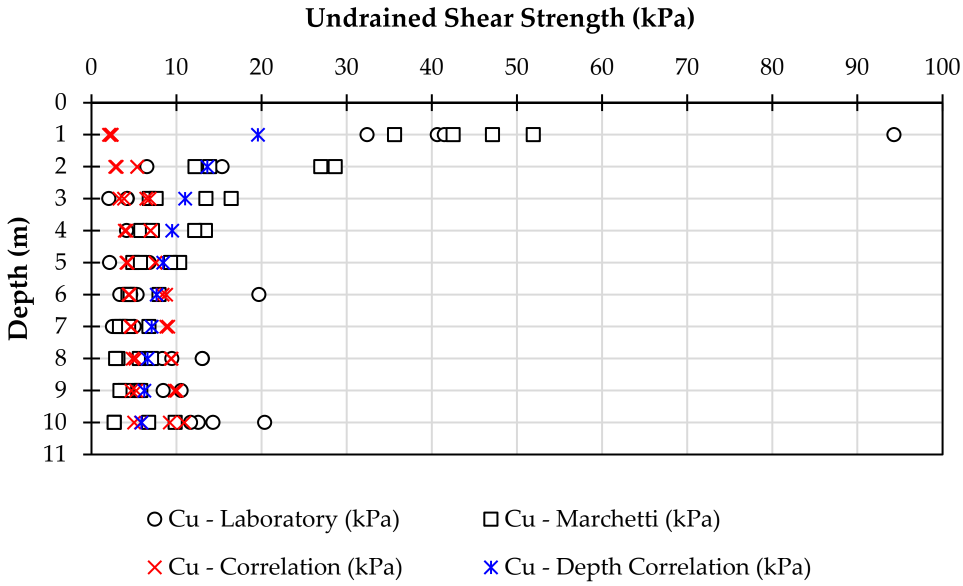

Figure 25. Comparison between different undrained shear strengths.

The tendency assumed by the values calculated with the equation obtained was notorious, because it kept C_u values in the order of 2 to 10 kPa, and they increased with depth. Although this equation could provide acceptable values for soft soils, it was not useful for more consistent soils. For example, in the first meter, where we had no organic soils, the C_u calculated from Equation (7) was less than the values obtained from the laboratory tests.

In addition, it was possible to observe that the trend generated from the laboratory results and depth (Equation (8)) presented higher values than those obtained in Equation (3) in meters 2, 3, and 4. However, from meter 5 to meter 10, it adapted better to the results obtained by the equation as a function of K_D and σ'_{vo}, as shown in Figure 25.

$$C_u = 19.548z^{-0.523} \tag{8}$$

where:

z: depth, m.

4.3. Density

Although Marchetti does not have a defined equation to obtain the density of soils, there is a nomogram that relates E_D and I_D and provides the relationship between soil density and water density (γ_s/γ_w). The nomogram presented in Figure 17 established that materials whose E_D value was less than 12 bar (1.2 MPa) are MUCK/PEAT, and regardless of the value taken by I_D, the ratio γ_s/γ_w would be 1.5. Assuming that the density of water was 1 g/cm^3, all soft material would have a density of 1.5 g/cm^3; however, this was not true.

Figure 11 showed that density values ranged from 1 to 1.30 g/cm^3 for this material of study. In addition, the soil E_D data did not reflect the density value that would be provided by the Marchetti plot. Considering all the previously mentioned parameters, it was decided to correlate the density values of the soil with its corresponding I_D, obtaining the following results.

$$\rho = 0.874 + 0.453I_D \text{ with } I_D \leq 1 \tag{9}$$

The regression shown in Figure 26 was performed using Minitab and presents an R^2 of 0.552, which means that the association has a strong degree of relationship [37]. The linear relationship presents that as the density increases, the value of I_D increases. In addition,

Figure 26 shows that most of the data are grouped in the expected values of both density and I_D.

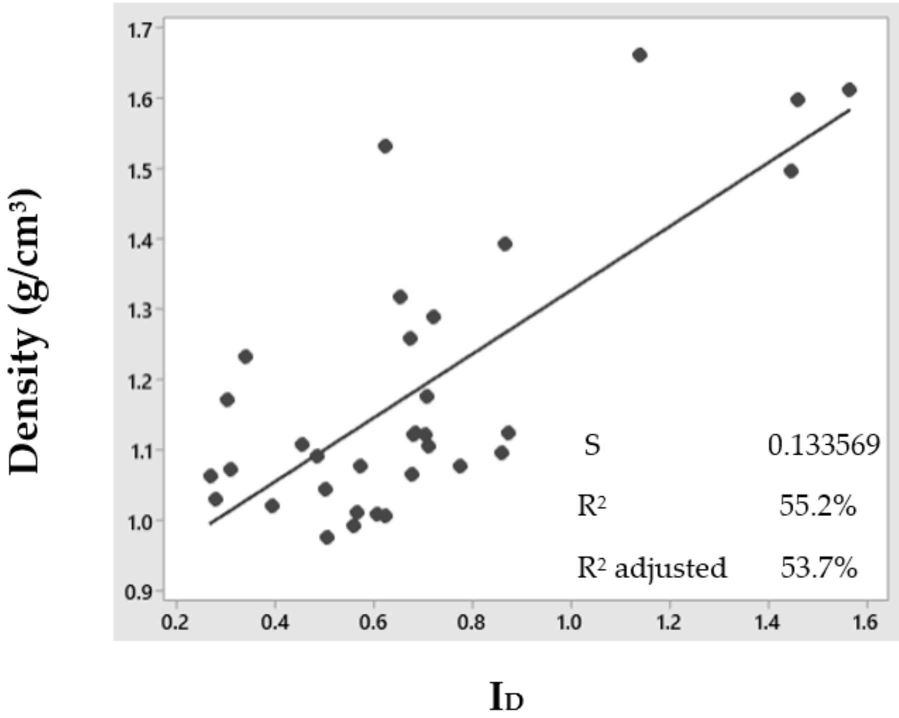

Figure 26. Correlation and regression between density and I_D value.

Additionally, the equation did not allow finding values lower than 1 g/cm^3, since this would be practically the density of water; however, for materials with an I_D lower than 0.278, the equation would provide values lower than 1 g/cm^3 since within the data contemplated in the regression, 2 samples presented this characteristic. However, it was necessary to develop new research for materials that have a density less than water's density.

Furthermore, Figure 27 shows that the density results obtained in the laboratory decrease with an increasing depth, presenting a potential tendency with an R^2 equal to 0.4018.

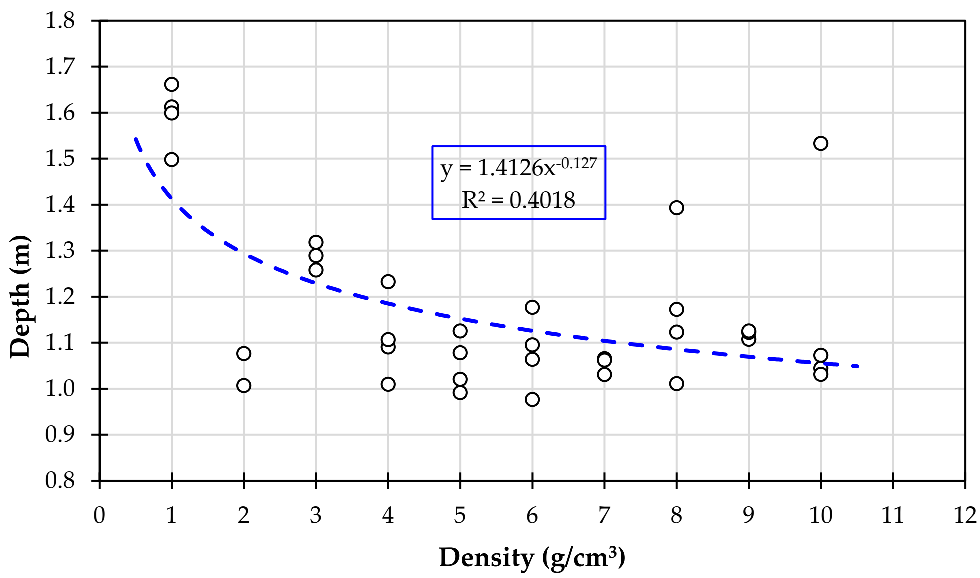

Figure 27. Correlation equation based on test results and depth for density.

In addition, as with the other two parameters, the density obtained in the laboratory, the density obtained with the Marchetti nomogram, considering a water density of 1 g/cm^3, and the density obtained with Equations (9) and (10) are compared in Figure 28.

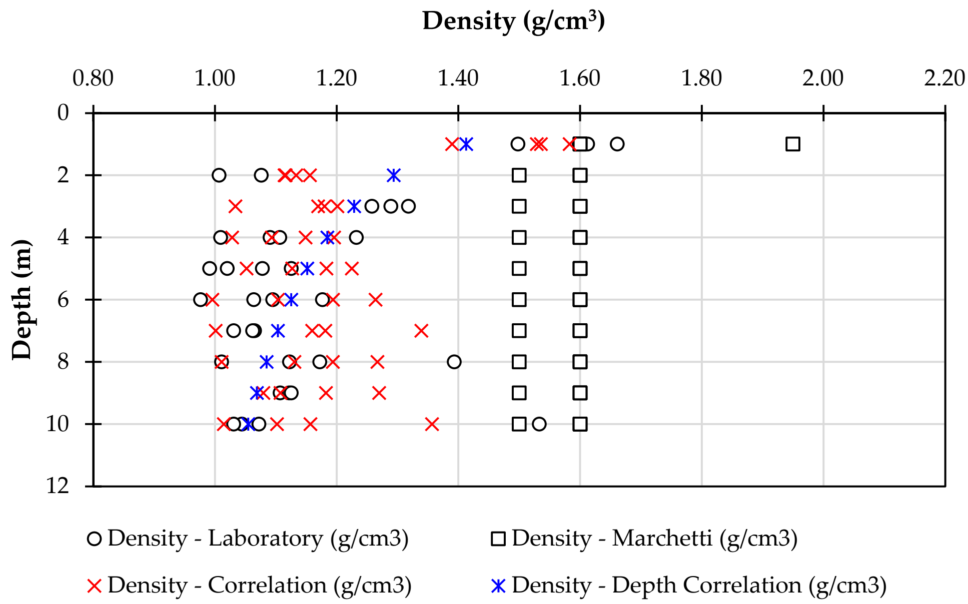

Figure 28. Comparison between density found by the Marchetti nomogram, density found by the equation in the previous graph, and density found in the laboratory.

The difference in the data obtained was notorious; the Equation (9) presented data as a function of I_D, which was close to the real density values. In this case, the use of Marchetti's method provided data that were not following the material that was obtained.

Moreover, it can be observed that the trend generated from the laboratory results and depth (Equation (10)) presented higher values than those obtained in Equation (3) in meter 2. However, from meter 3 to 10, it presented intermediate results, with respect to the results obtained by the equation as a function of the I_D, as shown in Figure 28.

$$\rho = 1.413z^{-0.127} \quad (10)$$

where:

z: depth, m.

4.4. Final Equations

In this study, the equations were obtained to find geomechanical parameters of the undrained shear strength (C_u), elasticity modulus (E), and density (ρ) for soft organic soils, presented in the "El Garrochal" sector, that are in Southern Quito. A summary of the derived expressions obtained as a function of the DMT parameters is shown in Table 8; while Table 9 is presented as a summary of equations as a function of the depth.

Table 8. Summary of equations obtained as a function of the DMT parameters.

Parameter	Units	Description	Equation	
E	MPa	Elasticity Modulus	$E = 0.231e^{0.326E_D}$	$I_D \leq 1$
C_u	kPa	Undrained Shear Strength	$C_u = 0.262\sigma'_{vo}K_D{}^{-0.221}$	$I_D \leq 1$
ρ	g/cm^3	Density	$\rho = 0.874 + 0.453I_D$	$I_D \leq 1$

Table 9. Summary of equations obtained as a function of depth.

Parameter	Units	Description	Equation
E	MPa	Elasticity Modulus	$E = 1.191z^{-0.581}$
C_u	kPa	Undrained Shear Strength	$c_u = 19.548z^{-0.523}$
ρ	g/cm^3	Density	$\rho = 1.413z^{-0.127}$

After reviewing the joint results between the correlations derived in this work and those presented by Marchetti, it was possible to affirm that there was a difference between both. First, the equations that were obtained provided more conservative values and, considering the nature of the material analyzed, this provided confidence regarding their use in engineering projects, which will be developed in the study sector. According to Mlynarek, Tschuschke, and Wierzbicki (2006) [38], Marchetti's expressions estimated these parameters very well in inorganic soils. However, organic soils and peat need study given their erratic composition.

In addition, it is important to mention that Figures 21, 25 and 28 showed that the results obtained by the equations presented in Table 8 presented values closer to the laboratory tests. While the equations in Table 9, which were developed as a function of depth, presented specific values for each meter which did not always adapt to the real laboratory results. However, the equations based on depth present similarity in the results obtained from meter 5 to meter 10.

Furthermore, it is important to mention that the results presented in the previously mentioned figures showed that the results provided by the Marchetti nomogram in the density estimation were higher than the real ones; therefore, this nomogram overestimated the density of the soils in the study area. Additionally, in Figure 25 we could observe that for the undrained shear strength, the results established based on the original Marchetti equations overestimated the real results in meter 2, 3 and 4, while they were slightly adjusted in the last 5 m.

Finally, Figure 21 showed that the values provided by the original Marchetti equation for obtaining the modulus of elasticity generated considerably higher results than those obtained in the laboratory, which reaffirmed that the Marchetti equations should be modified according to the specific soils of each region.

5. Conclusions

The equations that were present in Table 8 were appropriate for soils present in the "El Garrochal" sector, in Southern Quito, which was composed of mostly organic material. The organic material presented in this type of soil is composed of a mix of decomposing organic materials, wooden roots, and inorganic soils, but in less quantity.

Therefore, it was necessary to adapt the DMT equations to obtain correlations that better approximate the natural in situ conditions of soft soils. However, it is important to talk about the individual results, which must compare them not only with the values obtained from correlations, but it is also important compare them with laboratory test results.

The most discussed parameter in this type of research was the undrained shear strength (C_u). Figure 17a showed that this parameter assumed values between 0 and 15 kPa, being the most critical zone between meters 2 and 7, with C_u less than 10 kPa of each well. Equation (6) showed a similar behavior in this section, taking conservative values without overestimating them; however, the values that were obtained by Marchetti's equation presented high values. Hence, the original Marchetti equation had to be modified to consider the organic character of the material, and for this reason, Marchetti's work provided better results in mineral soils [39].

As with the undrained shear, the modulus of elasticity obtained by Equation (3) provided values that were closer to those obtained in the laboratory (Figure 22), estimating better this parameter in organic soils. Therefore, because of the close relationship between these two parameters and the complexity of organic soils, it is worthwhile to carry out studies on this type of material.

In addition, Konkol, et al. (2019) [40] corroborated that Marchetti's expressions overestimated the undrained shear value in organic soils, showing how Marchetti's nomogram provided a bad classification of organic soils and does not allow for finding adequate density values. This can be verified in Figure 28, although the in situ density did not have a defined trend given the composition of the material, the nomogram provided data that did not reflect the conditions of the material in its natural state. Although Equation (9) had an erratic trend, it allowed for obtaining data more following the natural state of samples. The density in this organic soil ranged between 1.00 and 1.60 g/cm^3; it is important to use this range and consider its variable behavior to understand why it is important to obtain low-density values [4].

As a summary, the equations obtained (Table 8) complement the work proposed by Marchetti, who was responsible for providing an adequate method for the study and determination of parameters in soft soils, such as those found in this work. However, it is important to adapt Marchetti's equations according to the soil types present in each region. The equations provided in Table 9 were considered an additional contribution to this research; however, it is recommended to complement this research specifically to determine the influence of depth on the deviation of the results obtained. Finally, the importance of obtaining accurate parameters for this type of soil was due to its poor mechanical properties, which hinders its use in construction projects.

Author Contributions: Conceptualization, J.A.-S.; methodology, J.A.-S. and J.M.; software, J.M.; validation, J.A.-S. and M.A.-M.; formal analysis, J.A.-S.; investigation, J.M.; resources, J.M.; data curation, J.A.-S., M.A.-M. and N.J.; writing—original draft preparation, N.J.; writing—review and editing, M.A.-M.; visualization, M.A.-M. and N.J.; supervision, J.A.-S.; project administration, J.A.-S.; funding acquisition, J.M. All authors have read and agreed to the published version of the manuscript.

Funding: This research received no external funding.

Institutional Review Board Statement: Not applicable.

Informed Consent Statement: Not applicable.

Data Availability Statement: Not applicable.

Acknowledgments: The authors acknowledge the Laboratory of Strength of Materials, Soil Mechanics, Pavements and Geotechnics and the staff of the Research Directorate from Pontificia Universidad Católica del Ecuador (PUCE) for their support during the development of this research.

Conflicts of Interest: The authors declare no conflict of interest.

References

1. Marchetti, S.; Marchetti, D.; Villalobos, F. El Dilatómetro Sísmico SDMT para ensayos de suelos in situ. *Obras Y Proy.* **2013**, 20–29. [CrossRef]
2. Marchetti, S.; Monaco, P.; Tonati, G.; Clabrese, M. *The Flat Dilatometer Test (DMT) in Soil Investigations*; International Society for Soil Mechanics and Geotechnical Engineering (ISSMGE): London, UK, 2001.
3. Sánchez, J.D.A. Determination of the undrained shear strength of organic soils using the Cone Penetration Test and Marchetti's Flat Dilatometer Test. *Puce* **2018**, *106*, 3–39.
4. Rabarijoely, S. A New Approach to the Determination of Mineral and Organic Soil Types Based on Dilatometer Tests (DMT). *Appl. Sci.* **2018**, *8*, 2249. [CrossRef]
5. Bandyopadhyay, K.; Das, K.; Nandi, S.; Halder, A. Dilatometer-an in Situ Soil Exploration Tool for Problematic Ground Conditions vis-à-vis for Economizing Construction Activities. *Indian Geotech. J.* **2022**, *52*, 1155–1170. [CrossRef]
6. Marchetti, S. Some 2015 Updates to the TC16 DMT Report 2001. In Proceedings of the 3rd International Conference on the Flat Dilatometer, Roma, Italy, 14–16 June 2015. Available online: www.marchetti-dmt.it (accessed on 11 July 2023).
7. Burlon, S.; Frikha, W.; Monaco, P. Session report: Pressuremeter and Dilatometer. In Proceedings of the 5th Geotechnical and Geophysical Site Characterization ISC'5, Sydney, Australia, 5–9 September 2016; pp. 259–269.

8. Amoroso, S.; Monaco, P.; Minarelli, L.; Stefani, M.; Marchetti, D. Estimation of geotechnical parameters by CPTu and DMT data: A case study in Emilia Romagna (Italy). In *Cone Penetration Testing 2018, Proceedings of the 4th International Symposium on Cone Penetration Testing (CPT'18), 21–22 June 2018, Delft, The Netherlands*; Hicks, M.A., Pisanò, F., Peuchen, J., Eds.; CRC Press: Boca Raton, FL, USA, 2018; pp. 85–91.
9. Monnet, J. Tests by Flat Dilatometer (DMT). In *In Situ Tests in Geotechnical Engineering*; John Wiley & Sons, Ltd.: Hoboken, NJ, USA, 2015; pp. 105–112. [CrossRef]
10. Shen, H.; Haegeman, W.; Peiffer, H. Instrumented DMT: Review and Analysis. In Proceedings of the 3rd International Conference on the Flat Dilatometer, Rome, Italy, 14–16 June 2015.
11. Berisavljevic, D.M.; Berisavljevic, Z.M. Dilatometer and seismic dilatometer tests in different depositional environments. In Proceedings of the 6th International Conference on Geotechnical and Geophysical Site Characterization (ISC2020), Budapest, Hungary, 7–11 September 2020.
12. Liu, X.-Y.; Zhu, D.; Yuan, D. Improvement and application of flat dilatometer. *Chin. J. Geotech. Eng.* **2013**, *35*, 1375–1380.
13. Benoı⨯t, J.; Stetson, K.P. Use of an Instrumented Flat Dilatometer in Soft Varved Clay. *J. Geotech. Geoenvironmental Eng.* **2003**, *129*, 1159–1167. [CrossRef]
14. Santander Vásquez, P.E. *Informe Técnico de Inspección Provincia de Pichincha-Quito Sector Turubamba*; Secretaría Nacional de Gestión de Riesgos: Quito, Ecuador, 2013.
15. *ASTM D1587-15*; Standard Practice for Thin-Walled Tube Sampling of Fine-Grained Soils for Geotechnical Purposes 1. ASTM International: West Conshohocken, PA, USA, 2015. [CrossRef]
16. *ASTM D2216-19*; Standard Test Method for Laboratory Determination of Water (Moisture) Content of Soil and Rock by Mass. ASTM International: West Conshohocken, PA, USA, 2019; pp. 1–5. [CrossRef]
17. *ASTM D4318-17*; Standard Test Methods for Liquid Limit, Plastic Limit, and Plasticity Index of Soils. ASTM International: West Conshohocken, PA, USA, 2017; Volume 4, pp. 1–14. [CrossRef]
18. *ASTM D1140-17*; Standard Test Methods for Determining the Amount of Material Finer than 75-µm (No. 200) Sieve in Soils by Washing. ASTM International: West Conshohocken, PA, USA, 2017; pp. 1–6.
19. *ASTM D2487-17*; Standard Practice for Classification of Soils for Engineering Purposes (Unified Soil Classification System) D2487-00. ASTM International: West Conshohocken, PA, USA, 2017; Volume 4, pp. 249–260.
20. *ASTM D2974*; Standard Test Methods for Determining the Water (Moisture) Content, Ash Content, and Organic Material of Peat and Other Organic Soils. ASTM International: West Conshohocken, PA, USA, 2020; pp. 1–4.
21. *ASTM D7263-21*; Standard Test Methods for Laboratory Determination of Density (Unit Weight) of Soil. ASTM International: West Conshohocken, PA, USA, 2021; Volume i, pp. 1–7.
22. *ASTM D2850-15*; Standard Test Method for Unconsolidated-Undrained Triaxial Compression Test on Cohesive Soils. ASTM International: West Conshohocken, PA, USA, 2015; Volume D2850−15, pp. 1–6.
23. Marchetti, S. In Situ Tests by Flat Dilatometer. *J. Geotech. Eng. Div.* **1980**, *106*, 299–321. [CrossRef]
24. *ASTM D6635-15*; Standard Test Method for Performing the Flat Plate Dilatometer 1. ASTM International: West Conshohocken, PA, USA, 2016. [CrossRef]
25. Larsson, R. *Dilatometerförsök. En In-Situ Metod för Bestämning av Lagerföljd Och Egenskaper i Jord. Dilatometer Test. An In-Situ Method for the Determination of Layer Sequences and Soil Properties*; Statens Geotekniska Institut: Linköping, Sweden, 1993.
26. Rabarijoely, S. New chart for classification of organic soils from dilatometer tests (DMT) results. *Ann. Warsaw Univ. Life Sci. SGGW* **2013**, *2*, 159–168. [CrossRef]
27. Cruz, N.; Cruz, J.; Rodrigues, C.; Cruz, M.; Amoroso, S. Behaviour of granitic residual soils assessed by SCPTu and other in-situ tests. In *Cone Penetration Testing 2018, Proceedings of the 4th International Symposium on Cone Penetration Testing, CPT 2018, Delft, The Netherlands, 21–22 June 2018*; Delft Univ Technol: Delft, The Netherlands, 2018; pp. 241–247.
28. Das, K.; Nandi, S.; Chattaraj, S.; Halder, A.; Sadhukhan, W. Estimation of subsoil parameters and settlement of foundation for a project in Kolkata based on CPT, DMT. *J. Phys. Conf. Ser.* **2022**, *2286*, 012026. [CrossRef]
29. Sutejo, Y.; Saggaff, A.; Rahayu, W.; Hanafiah. Physical and chemical characteristics of fibrous peat. *AIP Conf. Proc.* **2017**, *1903*, 090006. [CrossRef]
30. *ASTM D653-22*; Standard Terminology Relating to Soil, Rock, and Contained Fluids. ASTM International: West Conshohocken, PA, USA, 2022. [CrossRef]
31. Rabarijoely, S.; Lech, M.; Bajda, M. Determination of relative density and degree of saturation in mineral soils based on in situ tests. *Materials* **2021**, *14*, 6963. [CrossRef]
32. Skempton, A.W.; Petley, D.J. Ignition Loss and other Properties of Peats and Clays from Avonmouth, King's Lynn and Cranberry Moss. *Geotechnique* **1970**, *20*, 343–356. [CrossRef]
33. Li, W.; O'Kelly, B.C.; Yang, M.; Fang, K.; Li, X.; Li, H. Briefing: Specific gravity of solids relationship with ignition loss for peaty soils. *Geotech. Res.* **2020**, *7*, 134–145. [CrossRef]
34. Head, K.H.; Epps, R.J. *Manual of Soil Laboratory Testing. Volume 3, Effective Stress Tests*; Whittles Publishing: Caithness, UK, 2014.
35. Briaud, J.L.; Spencer, J. Introduction to Soil Moduli. *Eotechnical News* **2001**, *19*, 54–58.
36. Akpila, B.; Omunguye, I. Soil Modulus and Undrained Cohesion of Clayey Soils from Stress-Strain Models. *Can. J. Pure Appl. Sci.* **2014**, *8*, 3155–3161.

37. Hernández Sampieri, R.; Fernández Collado, C.; Baptista Lucio, P. *Metodología de la Investigación*; McGraw Hill: New York, NY, USA, 2014.
38. Wierzbicki, J. Evaluation of deformation parameters of organic subsoil by means of CPTU, DMT, SDMT. *Archit. Civ. Eng. Environ.* **2013**, *4*, 53–60.
39. Lechowicz, Z.; Fukue, M.; Rabarijoely, S.; Sulewska, M.J. Evaluation of the undrained shear strength of organic soils from a dilatometer test using artificial neural networks. *Appl. Sci.* **2018**, *8*, 1395. [CrossRef]
40. Konkol, J.; Międlarz, K.; Bałachowski, L. Geotechnical characterization of soft soil deposits in Northern Poland. *Eng. Geol.* **2019**, *259*, 105187. [CrossRef]